

# PARTICULARITIES OF THE NEGATIVE STREAMER PROPAGATION IN HOMOGENEOUS AND INHOMOGENEOUS ELECTRIC FIELDS. COMPUTER SIMULATION

*O.V. Manuilenko, V.I. Golota*

*NSC “Kharkov Institute of Physics and Technology”, Kharkov, Ukraine*

*E-mail: ovm@kipt.kharkov.ua*

The results of numerical simulations of negative streamer propagation in nitrogen in the plane - to - plane and the needle - to - plane geometries are presented. Computer simulations has been performed by finite element method, which allows to accurately describe the boundaries of complicated shape. It is shown that the propagation velocity of the negative streamer in a nonuniform electric field (the needle - to - plane geometry) is always greater than its velocity in a uniform field (the plane - to - plane geometry) at the same electrical potentials on the electrodes. It is shown that with decreasing curvature radius of the needle the streamer propagation velocity increases. The growth of the streamer speed, with decreasing of the needle curvature radius, is stopped when the needle curvature radius reaches a certain critical size. It is shown that in the region of the strong nonlinearity, when the dynamics of the streamer propagation is determined by the space charge, its velocity as a function of the longitudinal coordinate is independent of the needle curvature radius.

PACS: 52.80.Mg, 52.80.Tn

## INTRODUCTION

Papers [1-5] are devoted to the numerical modeling of the negative streamer in nitrogen within the drift-diffusion approximation. These works are used, with the exception of [5], the regular nonadaptive meshes to solve the continuity and Poisson equations. Streamer is a nonlinear structure with a sharp edge. Therefore, for its correct resolution in numerical simulations were used the exponential representation for the current density in the drift-diffusion approximation – the Scharfetter-Gummel algorithm [1,2], or numerical schemes with adaptation of a regular grid [5]. Regular meshes, as opposed to irregular grids, which are used in the finite element method, can not accurately describe the arbitrary boundaries of complex shape, such as the geometry of the needle - to - plane. Therefore, in [1-5] were performed numerical modeling of the negative streamer in nitrogen in a uniform electric field (the plane - to - plane geometry). In this paper the results of numerical simulations, using the finite element method, of negative streamer propagation in nitrogen in the plane - to - plane and needle - to - plane geometries are presented.

## SIMULATION RESULTS

The set of equations describing the propagation of the negative (anode - directed) streamer in nitrogen is:

$$\frac{\partial n_e}{\partial t} + \nabla \cdot (-n_e \mu_e \vec{E} - D_e \nabla n_e) = S_{iz}, \quad (1)$$

$$\frac{\partial n_i}{\partial t} + \nabla \cdot (n_i \mu_i \vec{E} - D_i \nabla n_i) = S_{iz}, \quad (2)$$

$$\nabla^2 V = \frac{e}{\epsilon_0} (n_e - n_i), \quad \vec{E} = -\nabla V, \quad (3)$$

where,  $n_e$  and  $n_i$  are electron and ion densities;  $\mu_e$ ,  $\mu_i$  are electron and ion mobilities;  $D_e$ ,  $D_i$  are diffusion coefficients for electrons and ions.  $V$  is electric potential,  $e$  is the absolute value of the electron charge,  $\epsilon_0$  is the permittivity of free space. Sources  $S_{iz}$  in the

right-hand sides of equations (1) and (2) represent the birth of electrons and ions by impact ionization:

$$S_{iz} = n_e \mu_e |\vec{E}| \alpha_o \exp(-E_o / |\vec{E}|), \quad (4)$$

where  $\alpha_o$  is the ionization coefficient,  $E_o$  is the threshold field for impact ionization. We did not include in the right sides of equations (1) and (2) other sources and sinks of charged particles, such as, for example, photoionization and recombination, as in the case of pure nitrogen, on the simulation time (streamer propagation time through the discharge gap), these sources and sinks are negligible compared to the impact ionization. Expression (4) allows the introduction of a set of natural scales: spatial scale  $l_o = 1/\alpha_o$ , scale for electric field  $E_o$ , scale for speed  $v_o = \mu_e E_o$ , time scale  $t_o = l_o / v_o$ , scale for diffusion  $D_o = l_o^2 / t_o$ , and density scale  $n_o = \epsilon_o \cdot E_o / (e \cdot l_o)$ . For nitrogen, under normal conditions,  $E_o = 197600$  V/cm,  $\alpha_o = 4332$  cm<sup>-1</sup>,  $\mu_e =$  cm<sup>2</sup>V<sup>-1</sup>s<sup>-1</sup>. Passing in (1)...(3) to dimensionless variables  $\vec{r} = \vec{r} / l_o$ ,  $t = t / t_o$ ,  $n_e = n_e / n_o$ ,  $n_i = n_i / n_o$ , we obtain:

$$\frac{\partial n_e}{\partial t} + \nabla \cdot (-n_e \vec{e} - D \nabla n_e) = n_e |\vec{e}| \exp\left(-\frac{1}{|\vec{e}|}\right), \quad (5)$$

$$\frac{\partial n_i}{\partial t} = n_e |\vec{e}| \exp\left(-\frac{1}{|\vec{e}|}\right), \quad (6)$$

$$\nabla^2 V = n_e - n_i \equiv -\rho, \quad \vec{e} = -\nabla V. \quad (7)$$

Ions in (6) further considered as immovable since their mobility several orders of magnitude smaller than the electron mobility, which allows, for the simulation time, neglect their displacement.

Fig. 1 shows the geometry of the computational domain, an example of mesh for solution of (5)-(7) and the boundary conditions. At start time, the electrons and ions with the same density, which are Gaussian distribu-

tions in space -  $n_e = n_i = \delta \cdot \exp(-\bar{r}^2 / \sigma)$ , placed in the area of the cathode,  $\delta = 10^{-4}$ ,  $\sigma = 100$ . Anode potential is  $V_0 = 128$ , which corresponds, for a flat geometry, to the dimensionless electric field at the initial time of 0.5 or 98 800 V/cm. Dimensionless diffusion coefficient is  $D = 0.1$ , which corresponds to  $1800 \text{ cm}^2\text{s}^{-1}$ . The other parameters are:  $L_z = 256$ ,  $L_r = 128$ ,  $H = 40$ ,  $R = \{5, 10, 20, 40, 80, 120, \text{inf} - \text{flat geometry}\}$ .

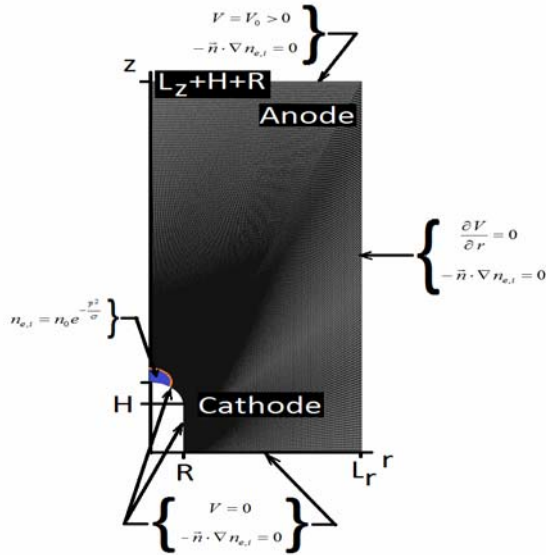


Fig. 1. Geometry of the computational domain and boundary conditions

Fig. 2 shows the  $z$ -coordinates of the maxima of the normalized electric field  $|\vec{\mathcal{E}}(r = 0, z; t)|^{\max}$  versus time for different radii of curvature of the needle -  $R = \{5, 10, 20, 40, 80, 120, \text{inf}\}$ . As can be seen from Fig. 2, for small radii of curvature of the needle ( $R \leq 20$ ), the dynamics of the streamer passing through the discharge gap is almost independent of the  $R$ , although a slight increase in the streamer velocity, with decreasing  $R$ , can be seen.

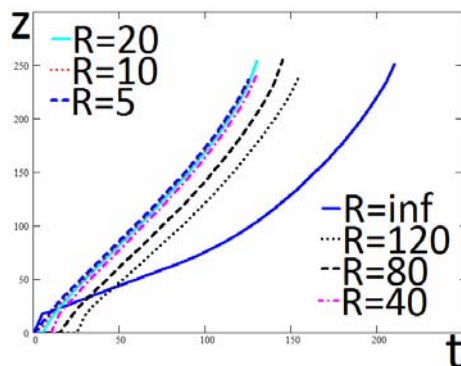


Fig. 2.  $z$ -coordinates of the maxima of the normalized electric field vs time for different needle radii  $R$

Fig. 3 shows the speed of the maximum  $|\vec{\mathcal{E}}|^{\max}$  depending on the time, which are the velocity of the

negative streamer ( $V_s$ ) in the discharge gap. Fig. 3 is obtained from Fig. 2 by means of direct numerical differentiation.

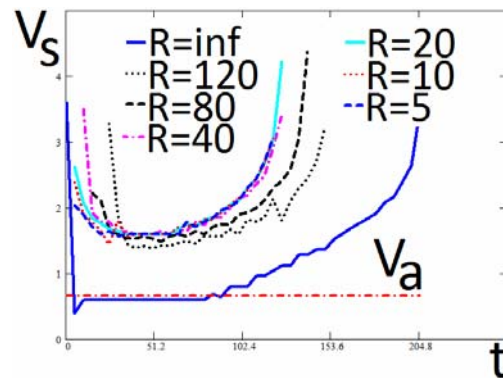


Fig. 3. Velocity of the negative streamer vs time for different needle radii  $R$

As can be seen from Fig. 3, the behavior of the streamer velocity  $V_s$  as a function of time has four characteristic regions: (1) a sharp drop in the beginning of the movement, (2) motion with constant velocity, and (3) the area of the first (low) acceleration, and (4) the area of the second (strong) acceleration. For a planar geometry, (1) and (2) represent the initial stage of an electron avalanche development, when the space charge is small, and the external electric field is not distorted by the space charge. Region (3) corresponds to the nonlinear stage of streamer propagation, when the magnitude of the space charge is significantly different from zero, and the external electric field is significantly distorted. Region (4) corresponds to the approach of the streamer to the anode, and to its exit through anode from the simulation domain. Solution of the linearized equations (5)...(7) in one dimension, for the velocity of the ionization wave gives:

$$V_a = |\varepsilon_0| + 2\sqrt{D|\varepsilon_0|\exp(-1/|\varepsilon_0|)}, \quad (8)$$

where  $\varepsilon_0$  is the external electric field, and  $D$  is the diffusion coefficient.  $V_a$  is shown in Fig. 3 by a straight line. Fig. 3 shows that, after a rather rapid transition process (region (1)), the streamer velocity  $V_s$  approaches to the asymptotic velocity  $V_a$  (region (2)), which corresponds to the linear stage of the avalanche development. The moment of transition avalanche to streamer can be defined as the time when the streamer velocity  $V_s$  begins to differ from asymptotic speed  $V_s$ , which corresponds to the end of the region (2). In the case of inhomogeneous fields, area (2) can not be identified with the linear stage of the development of the avalanche, because the effect of space charge appears much earlier. As can be seen from Fig. 3, when the needle curvature radii  $R \leq 20$ , in (2)–(4) the speed of the streamer  $V_s$  does not significantly increase with decreasing  $R$ .

Fig. 4 shows the velocity of the negative streamer  $V_s$  versus longitudinal coordinate  $z$ . It is seen that in the strong non-linearity regions (areas (3), and (4)) the speed of the streamer  $V_s$  as a function of longitudinal coordinate  $z$  is independent of the needle radius  $R$ . This

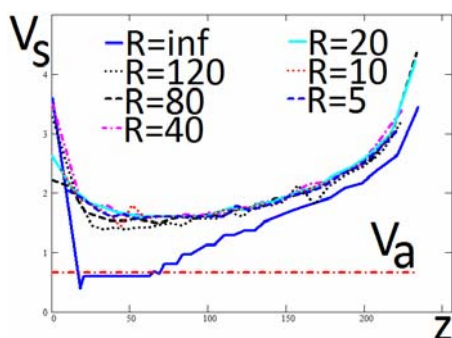


Fig. 4. Velocity of the negative streamer vs longitudinal coordinate  $z$  for different needle radii  $R$

can be explained with screening of the electric field of the needle by the space charge of the streamer.

### CONCLUSIONS

The paper presents the results of numerical simulations the propagation of a negative streamer in nitrogen in the plane - plane and the needle - plane geometries. Computer simulations has been performed by finite element method, which allows to accurately describe the boundaries of complicated shape. It is shown that the propagation velocity of the negative streamer in a nonuniform electric field (the needle - plane geometry) is always greater than its velocity in a uniform field (the plane - plane geometry) at the same potentials on the electrodes. It is shown that the

behavior of the streamer velocity versus time has four specific areas: (1) a sharp drop at the beginning of the movement, (2) propagation with a constant velocity, (3) the area of the first (weak) acceleration, and (4) the area of the second (strong) acceleration at the approach of the streamer head to the anode. It is shown that with decreasing curvature radius of the needle the streamer propagation velocity increases. The growth of the streamer speed, with decreasing of the needle curvature radius, is stopped when the needle curvature radius reaches a certain critical size. It is shown that in the region of the strong nonlinearity, when the dynamics of the streamer propagation is determined by the space charge, its velocity as a function of the longitudinal coordinate is independent of the needle curvature radius.

### REFERENCES

1. A.A. Kulikovskiy. The structure of streamers in N<sub>2</sub>. I. fast method of space-charge dominated plasma simulation // *J.Phys.D: Appl.Phys.* 1994, v. 27, p. 2556-2563.
2. A.A. Kulikovskiy. The structure of streamers in N<sub>2</sub>. II. Two-dimensional simulation // *J.Phys.D: Appl.Phys.* 1994, v. 27, p. 2564-2569.
3. A.A. Kulikovskiy. Two-dimensional simulation of the positive streamer in N<sub>2</sub> between parallel-plate electrodes // *J.Phys.D: Appl.Phys.* 1995, v. 28, p. 2483-2493.
4. M. Arrayás, U. Ebert, W. Hundsdorfer. Spontaneous branching of anode-directed streamers between planar electrodes // *Phys. Rev. Lett.* 2002, v. 88, p. 174502.
5. C. Montijn, W. Hundsdorfer, U. Ebert. An adaptive grid refinement strategy for the simulation of negative streamers // *J. Comp. Phys.* 2006, v. 219, p. 801-835.

Article received 11.10.12

## ОСОБЕННОСТИ РАСПРОСТРАНЕНИЯ ОТРИЦАТЕЛЬНОГО СТРИМЕРА В ОДНОРОДНОМ И НЕОДНОРОДНОМ ЭЛЕКТРИЧЕСКИХ ПОЛЯХ. ЧИСЛЕННОЕ МОДЕЛИРОВАНИЕ

О.В. Мануйленко, В.И. Голота

Приведены результаты численного моделирования методом конечных элементов распространения отрицательного стримера в азоте в геометриях плоскость–плоскость и игла–плоскость. Показано, что скорость распространения стримера в неоднородном поле (геометрия игла–плоскость) всегда больше его скорости в однородном поле (геометрия плоскость–плоскость) при одинаковых потенциалах на электродах. Показано, что при уменьшении радиуса кривизны иглы скорость распространения стримера возрастает. Рост продолжается до некоторого критического радиуса, после которого рост скорости стримера практически прекращается. Показано также, что в области сильной нелинейности, когда динамика распространения стримера определяется его объемным зарядом, его скорость, как функция продольной координаты, не зависит от радиуса кривизны иглы.

## ОСОБЛИВОСТІ РОЗПОВСЮДЖЕННЯ НЕГАТИВНОГО СТРИМЕРА В ОДНОРІДНИХ І НЕОДНОРІДНИХ ЕЛЕКТРИЧНИХ ПОЛЯХ. ЧИСЛОВЕ МОДЕЛЮВАННЯ

О.В. Мануйленко, В.И. Голота

Наведено результати числового моделювання методом кінцевих елементів поширення негативного стримера в азоті в геометріях площина–площина і голка–площина. Показано, що швидкість поширення стримера в неоднорідному полі (геометрія голка–площина) завжди більше його швидкості в однорідному полі (геометрія площина –площина) при однакових потенціалах на електродах. Показано, що при зменшенні радіуса кривизни голки швидкість розповсюдження стримера зростає. Зростання триває до деякого критичного радіуса, після якого зростання швидкості стримера практично припиняється. Показано також, що в області сильної нелінійності, коли динаміка розповсюдження стримера визначається його об'ємним зарядом, його швидкість, як функція поздовжньої координати, не залежить від радіуса кривизни голки.